

A Molecular Dynamics Simulation Study of Relaxation Processes in the Dynamical Fast Component of Miscible Polymer Blends

Dmitry Bedrov* and Grant D. Smith

Department of Materials Science and Engineering and Department of Chemical Engineering,
University of Utah, 122 S. Central Campus Dr., Rm. 304, Salt Lake City, Utah 84112

Received August 4, 2005; Revised Manuscript Received October 1, 2005

ABSTRACT: Molecular dynamics simulations of model miscible polymer blends consisting of 1,4-polybutadiene (PBD) (slow component) and PBD chains with reduced or eliminated dihedral barriers (fast component) have been performed in order to study the influence of blending on segmental relaxation processes in the fast component. We find that blending with a slow (high glass transition temperature, or T_g) component significantly increases the separation between the α - and β -relaxations of the fast (low T_g) component, which may be unresolvable or nearly unresolvable in the pure melt. The α -relaxation of the fast component is strongly influenced by blending, moving to longer relaxation times with increasing concentration of the slow component. In contrast, the relaxation time of the β -process of the fast component is only weakly influenced by blending. We speculate that this separation of relaxations processes in the fast component with blending can explain segmental relaxation behavior observed in dielectric and NMR relaxation studies of miscible polymer blends with disparate component dynamics.

I. Introduction

Despite extensive study, the underlying mechanisms responsible for dynamics in miscible polymer blends remain poorly understood, and the interpretation of polymer blend dynamics remains controversial. A prime example of such controversy is the segmental relaxation of the lower glass transition temperature or T_g (dynamically fast) component in blends comprised primarily of the higher T_g (dynamically slow) component. Dielectric measurements of such blends reveal significant dielectric loss at high frequency that exhibits weak concentration dependence and is located in a frequency range similar to the response of the neat melt of the lower T_g component. In blends where the lower T_g component dominates the dielectric activity of the blend the dielectric loss of the blend (and hence the lower T_g component) was found to show either a very broad single relaxation or sometimes two distinct relaxations. For example, in polymer blends consisting of components with very different glass transition temperatures in the neat melts ($\Delta T_g > 80$ °C) such as polystyrene/poly(methylphenylsiloxane) (PS/PMPS)¹ or polystyrene/poly(vinyl methyl ether) (PS/PVME),^{2,3} dielectric spectroscopy has clearly showed two distinct relaxations of the fast component (PMPS and PVME). One relaxation was found to have a relaxation time similar to that of the neat melt of the fast component and another closer to that expected on the basis of blend average dynamics. Interpretations of dielectric measurements in blends with dynamically less asymmetric components ($\Delta T_g < 80$ °C) such as polyisoprene/poly(vinylethylene) (PI/PVE) have also resulted in apparently contradictory conclusions regarding the influence of blending on the dynamics of the fast component (PI). Alvarez et al.⁴ reported that they need to assume a bimodal relaxation of the PI component in the PI/PVE blend to interpret their data, while Kamath et al.⁵ and Arbe et al.⁶ claim that they were able to fit the dielectric response of the PI/PVE blend using unimodal relaxation for both components.

An additional controversy in understanding segmental relaxation of the fast component in miscible polymer blends apparently stems from the quite different relaxation time scales accessible to various experimental probes of segmental relaxation. QENS and NMR spin-lattice relaxation measurements are primarily sensitive to motions on the nanosecond or subnanosecond time scale while 2D-NMR measurements typically probe motions on the millisecond time scale. Dielectric spectroscopy has the broadest time window, ranging from nanoseconds to multiple seconds, but is most straightforwardly applied in the millisecond to microsecond domain. As a result of the differences in relaxation time scales various techniques are often utilized in study of the same blend at the quite different temperatures that are needed to bring the segmental relaxation time into the relaxation time scale of the particular experiment. The combination of different time scales and measurement at different temperatures can lead to apparently contradictory conclusions. For example, in the PI/PVE blend, the PI segmental relaxation times obtained from 2D-NMR measurements⁷ around 240 °C were estimated to be 2–3 orders of magnitude slower than in the neat PI melt, while QENS measurements⁶ at 270 °C suggested that PI segmental relaxation is barely affected by blending.

Several theoretical models attempt to explain dynamical behavior of blends and their components based on thermally driven concentration fluctuations,⁸ chain connectivity,⁹ or a combination of both.^{1,5,7,10} In these models, the local (segmental) dynamics of a polymer chain are thought to be determined by the local environment which deviates from the average blend composition. The Lodge–McLeish model⁹ suggests that segmental dynamics are defined by the environment on the scale of the Kuhn length. On this length scale chain connectivity results in a local environment for a polymer segment that is richer in segments of its own type than the average blend composition. While this model has not been applied to describe bimodal relaxation of the lower T_g component observed in some blends relatively

* Corresponding author. E-mail: bedrov@tacitus.mse.utah.edu.

dilute in the fast component, it does not exclude these phenomena. For polymers with large self-concentration or with segmental dynamics controlled by a local environment that is significantly smaller than the Kuhn length, it is possible, in the frame of this model, to have segments of the lower T_g component in two very different environments: one almost exclusively comprised of like segments and the other almost a 50/50 mixture of segments, which would lead to bimodal relaxation of the fast component.⁹

Models based on concentration fluctuations assume that segmental dynamics are determined by a local region that can be spontaneously rich in segments of either blend component. The size of this local region is related to cooperatively rearranging volumes associated with the glass transition¹¹ and (depending on the model) has certain temperature and composition dependences. Therefore, according to this class of models, a segment of each component can have a broad distribution of local environments (ranging from pure meltlike to dilute limits) on length scales of several nanometers that consequently leads to a broad dynamical response of the components and the blend. This type of model has been invoked to describe the dielectric relaxation of various blends including the bimodal relaxation of the lower T_g component.^{1,5,10} While concentration fluctuation-based models can qualitatively account for the presence of the bimodal relaxation in the fast component they are unable to describe the wide separation of relaxation times observed in experiments.^{1,5} A very recent attempt to use a concentration fluctuation model to describe the dielectric loss of PI/PVE blends resulted in a prediction of a much narrower dielectric loss than that obtained from experiments and completely missing a high-frequency wing in the blend dielectric loss.¹⁰

In summary, the theoretical models described above attempt to explain the dynamical response of miscible polymer blends and the perplexing behavior of the lower T_g component by considering heterogeneity in the composition of the local environment of polymer segments and local structure (e.g., density fluctuations, chain connectivity, etc.). While it has been shown that parameters of these models can be fitted to quantitatively reproduce composition and temperature dependence of segmental relaxation times for a variety of miscible polymer blends,^{5,9,12,13} there are a number of blends in which these models are able to predict only qualitative trends observed in experiments⁵ or fail completely.¹² The majority of those failures are associated with prediction of the fast component dynamics in the blend.

In this paper, we discuss segmental relaxation in model realistic polymer blends consisting of components with very different neat melt dynamics as obtained from molecular dynamics (MD) simulations. We believe that the relaxation mechanisms observed in this work are qualitatively generic and have not been considered before in interpretation of the segmental dynamics of the fast component of miscible polymer blends.

II. Simulation Methodology and Systems Investigated

Chemically realistic 1,4-polybutadiene (PBD) chains (or CR-PBD) have been represented using a quantum chemistry-based united atom force field.¹⁴ A detailed description of the CR-PBD model and extensive comparison of melt simulations with NMR spin-lattice

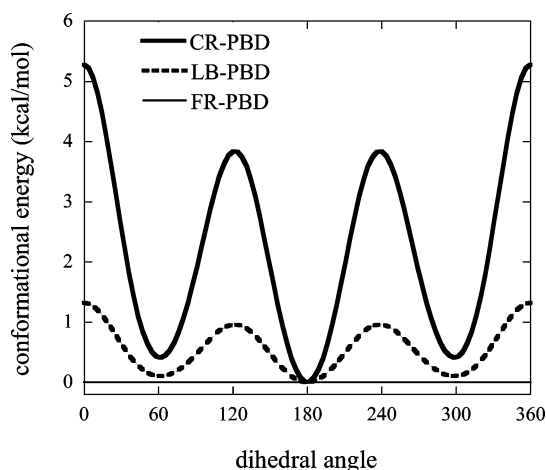


Figure 1. Dihedral energy profiles for the $C(sp^2)-C(sp^3)-C(sp^3)-C(sp^2)$ dihedral in CR-PBD, LB-PBD, and FR-PBD models.

relaxation,¹⁵ dynamic neutron scattering,¹⁶ and dielectric relaxation¹⁷ measurements can be found in the literature. To create components with faster dynamics two models have been employed. In the first model, the dihedral barriers of all backbone dihedrals (excepting double bonds) were reduced by a factor of 4 relative to the CR model (we refer to this model as low barrier chains or LB-PBD). In the second model, all backbone dihedrals have been eliminated completely, providing us with freely rotating chains or FR-PBD. In Figure 1, we compare the dihedral energy profiles for these models for the backbone $C(sp^2)-C(sp^3)-C(sp^3)-C(sp^2)$ torsion. All other bonded and nonbonded interactions in these three models are identical. Our previous simulations of FR-PBD melts¹⁸ have already demonstrated that the reduction or elimination of dihedral barriers in PBD melt allows essentially identical structural properties to those obtained using the CR-PBD model—only dynamic properties are influenced by the removal of the dihedral barriers. On the basis of Vogel–Fulcher fits to the temperature dependence of the α -relaxation time obtained from the torsional autocorrelation function (see below), we obtain glass transition temperatures¹⁹ of 170, 102, and 55 K for the CR-PBD, LB-PBD, and FR-PBD, respectively. Finally, to model a matrix that has much slower dynamics than CR-PBD we used heavy FR-PBD, further referred to as HFR-PBD. In HFR-PBD the atomic masses of FR-PBD chains have been increased by a factor of 2×10^{10} , thereby effectively shifting the relaxation time scales by 5 orders of magnitude to longer time. Note that qualitatively relaxation of the HFR-PBD melt is identical to that in FR-PBD; only the time scales are offset proportionally to $m^{1/2}$.

All blends consisted of 40 chains each having 30 repeat units. Bonds were constrained using the SHAKE algorithm.²⁰ A cutoff radius of 10 Å was used for truncation of van der Waals interactions. A multiple time step integrator with 1 fs time step for integration of bonded degrees of freedom (bonds and torsions) and 5 fs time step for nonbonded (intermolecular and intramolecular separated by five bonds and more) interactions was employed. Original configurations were taken from existing well-equilibrated CR-PBD melts trajectories obtained from our previous simulations. The desired fraction of chains was converted to FR-PBD, LB-PBD, or HFR-PBD and subsequently equilibrated

over 40 ns followed by production run over 200–400 ns using NVT ensemble molecular dynamics (MD) simulations. The following blends have been investigated: (a) FR-PBD/CR-PBD at 198 K with 10, 25, 50, 75, and 90% FR-PBD; (b) LB-PBD/CR-PBD at 198 K with 10, 25, 50, and 75% LB-PBD; and (c) CR-PBD/HFR-PBD at 500 K with 10% CR-PBD.

III. Results

A. Torsional Autocorrelation Function and Segmental Relaxation. The torsional autocorrelation (TACF), defined as

$$\text{TACF}(t) = \frac{\langle \theta(t)\theta(0) \rangle - \langle \theta(0) \rangle^2}{\langle \theta(0)^2 \rangle - \langle \theta(0) \rangle^2} \quad (1)$$

where θ is the absolute value of the dihedral angle ranging from 0 to π , was determined for the C(sp²)–C(sp³)–C(sp³)–C(sp²) dihedrals. For polymers with local dipole moments perpendicular to the chain backbone, such as 1,4-PBD, dielectric relaxation is closely related to the decay of the TACF. In this work, we use the TACF as a convenient measure of segmental scale relaxations in miscible polymer blends. Recently, we showed that FR-PBD²¹ and LB-PBD²² melts exhibit two-step decay (neglecting librations) in the TACF with increasing separation between the relaxation processes with decreasing temperature. Hence, an important consequence of the reduction (LB-PBD) or elimination (FR-PBD) of dihedral barriers beyond the lowering of characteristic relaxation times is the clear resolution of α - and β -relaxations of the backbone dihedrals within the time window accessible for MD simulations. Mechanistically, we found that the β -relaxation is due to large-scale conformational motions that are spatially homogeneous (all dihedrals visit each conformational state). However, on the time scale of the β -relaxation dihedrals while visit all conformational states cannot populate them with equilibrium probabilities due to packing constraints imposed by the surrounding matrix. Complete segmental relaxation (α -relaxation) occurs on longer time scales over which all dihedrals able to populate each conformational state with equilibrium probability, a process that requires cooperative motion of the matrix. A detailed discussion of molecular mechanisms responsible for the splitting of the α - and β -relaxations in the FR-PBD and LB-PBD melts can be found in refs 21 and 22.

In parts a and b of Figure 2 we show the TACF of the fast component (FR-PBD and LB-PBD) at selected blend compositions for the FR-PBD/CR-PBD and LB-PBD/CR-PBD blends, respectively. For reference, the TACF α -relaxation time for the CR-PBD melt is on the order of several microseconds, while the TACF α -relaxation times for the FR-PBD and LB-PBD melts are 48 and 840 ps, respectively. Both the FR-PBD and LB-PBD melts exhibit a weak separation between α - and β -relaxations at 198 K. As dynamically slow CR-PBD is blended with the fast component, we can see that the first step (excluding librations) in the decay of the TACF, or β -relaxation, of the fast component is at most weakly dependent on blend composition while the α -relaxation is clearly strongly dependent on blend composition.

We assume that both relaxations (α and β) in the TACF can be represented by the KWW function²³

$$f(t) = \exp\left[-\left(\frac{t}{\tau}\right)^\beta\right] \quad (2)$$

where τ is an apparent relaxation time and β is a stretching exponent. The TACFs for the fast components were fit using the Williams ansatz:²⁴

$$\text{TACF}(t) = A_\beta f_\beta(t) f_\alpha(t) + A_\alpha f_\alpha(t) \quad (3)$$

where $f_\alpha(t)$ and $f_\beta(t)$ are KWW functions representing the α - and β -relaxations, respectively, while A_α and A_β are amplitudes of these processes with the constraint $A_\alpha + A_\beta \leq 1.0$. The ansatz in eq 3 has been extensively used to fit relaxations where two statistically independent processes are both contributing in the same time domain.²⁵ Only data for $t > 1.0$ ps have been used in the fits. Integrated relaxation times for each process were determined from the time integral of the corresponding relaxation function $f_i(t)$ from zero to infinity.

Figure 3a shows relaxation times for the α - and β -relaxations of the fast component in the FR-PBD/CR-PBD and LB-PBD/CR-PBD blends as a function of blend composition. Figure 3a clearly shows that as the concentration of the slow component increases, the separation between α - and β -relaxations of the fast component increases dramatically due to the dramatic influence of blend composition on the α -relaxation and the insensitivity of the β -relaxation on blend composition. Figure 3b illustrates the composition dependence of the amplitude (A_α in eq 3) for the α -relaxation of the TACF for the fast component in the FR-PBD/CR-PBD and LB-PBD/CR-PBD blends. The weak composition dependence of the amplitudes indicates that the strengths of α - and β -relaxations of the fast component are not strongly affected upon blending. A more detailed discussion of the temperature and composition dependence of relaxation times, amplitudes, and stretching exponents of both relaxation processes in the slow and fast components in these blends will be addressed in the upcoming paper.

B. Dielectric Relaxation. Linear response theory allows us to obtain the complex dielectric permittivity $\epsilon(\omega) = \epsilon'(\omega) + i\epsilon''(\omega)$ using the relationship²⁶

$$\frac{\epsilon'(\omega) + i\epsilon''(\omega)}{\Delta\epsilon} = 1 - i\omega \int_0^\infty \Phi(t) \exp(-i\omega t) dt \quad (4)$$

where the dipole moment autocorrelation function (DACF) is given as

$$\Phi(t) = \frac{\langle M(0) \cdot M(t) \rangle}{\langle M(0) \cdot M(0) \rangle} = \frac{\sum_{i=1}^N \langle M_i(0) \cdot M_j(t) \rangle}{\sum_{i=1}^N \langle M_i(0) \cdot M_j(0) \rangle} \quad (5)$$

Here $M(t)$ and $M_i(t)$ are the dipole moment of the system and the dipole moment of chain i at time t , respectively, and N is the number of chains. For purposes of determining $M(t)$ we assume that the dipole moment of each polymer chain is uncorrelated with that of the other polymer chains.¹⁷ For the purpose of calculating the DACF hydrogen atoms were added to the united atom trajectories in the manner described previously,²⁷ and partial atomic charges have been subsequently assigned as described elsewhere.¹⁷

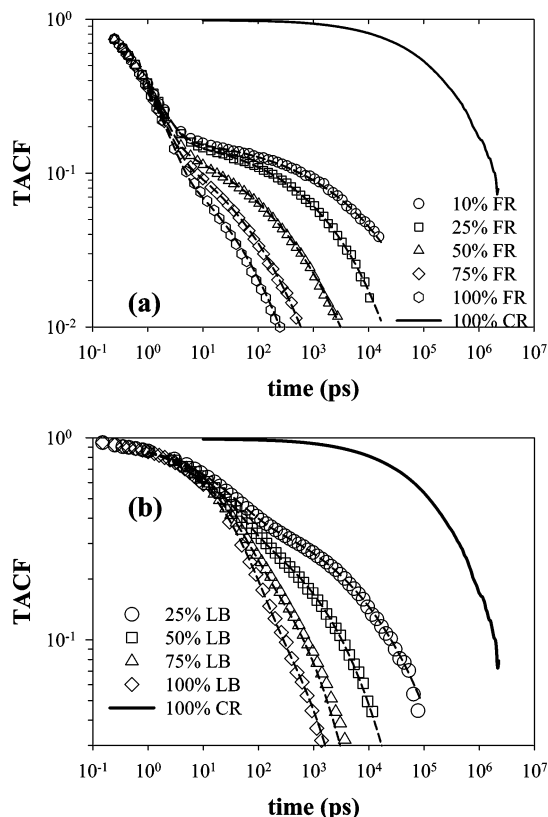


Figure 2. TACFs for the (a) FR-PBD in the FR-PBD/CR-PBD blend and (b) LB-PBD in the LB-PBD/CR-PBD blend as a function of concentration at 198 K. Also shown is the TACF of the CR-PBD melt at 198 K. Dashed lines show fits to eq 3.

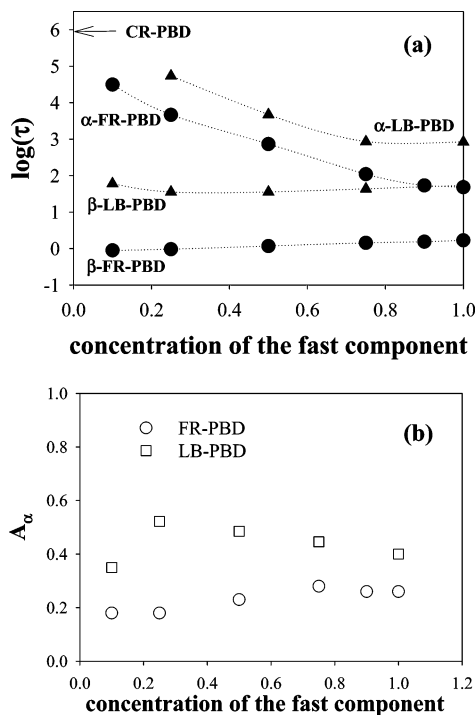


Figure 3. Concentration dependence of the (a) integrated relaxation times for the TACF α - and β -processes and (b) amplitudes for the α -process of the FR-PBD and LB-PBD components in the FR-PBD/CR-PBD and LB-PBD/CR-PBD blends.

In Figure 4 we show the DACFs of the LB-PBD component in the LB-PBD/CR-PBD blends as a function of concentration at 198 K. Similar to the TACFs the DACFs for LB-PBD show increasing separation between

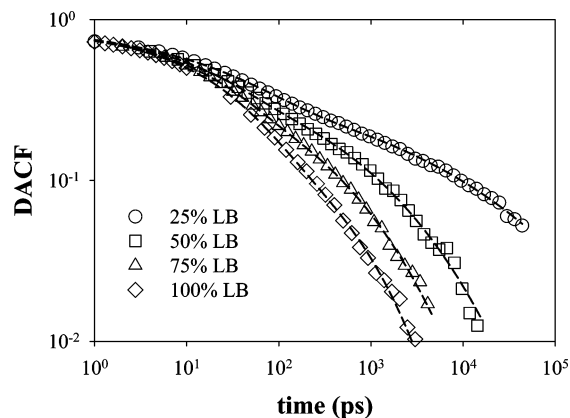


Figure 4. DACFs of the LB-PBD component in the LB-PBD/CR-PBD blends as a function of concentration at 198 K. Dashed lines show fits to eq 3.

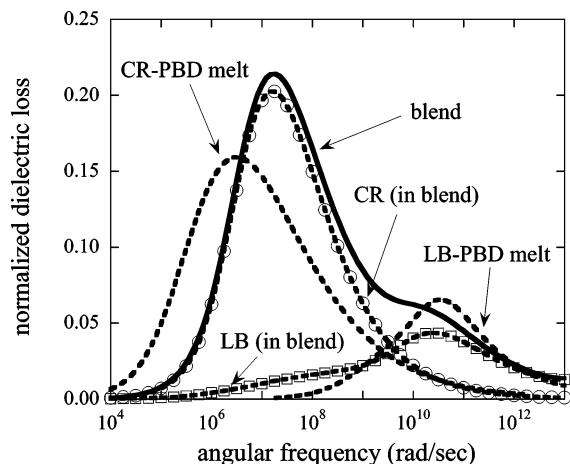


Figure 5. Dielectric loss as a function of frequency for the LB-PBD/CR-PBD blend and its components for the 25% LB-PBD concentration at 198 K. Also shown are dielectric losses for neat LB-PBD and CR-PBD melts scaled by their composition in the blend.

two relaxation processes with increasing concentration of the slow components. Fits of the DACFs by eq 3 are also shown in Figure 4. The composition dependence of the relaxation times for the α - and β -relaxations is similar to that seen for the relaxation times for the TACF shown in Figure 3a.

We have calculated dielectric response of the blend and its components for the LB-PBD/CR-PBD mixtures utilizing eq 4. In Figure 5, we show the normalized dielectric loss as a function of frequency for the components and total of the blend with 25% concentration of the LB-PBD component. Also shown are the dielectric losses for pure CR-PBD and LB-PBD melts weighted by 0.75 and 0.25, respectively. The weighting of the pure melts response facilitates comparison with the response of individual components in the blend. Examination of Figure 5 results in several striking observations. First, the dielectric response of the LB-PBD component in the blend shows two distinct peaks consistent with the split between the α - and β -relaxations observed in the TACFs and DACFs. The position of the high-frequency peak coincides with the peak position of dielectric loss in the pure LB-PBD melt, which consists of contributions of two processes that are separated only by about an order of magnitude in frequency yielding a single broad peak. The low frequency (α -relaxation) process for the LB-PBD component of the blend shows up as a very

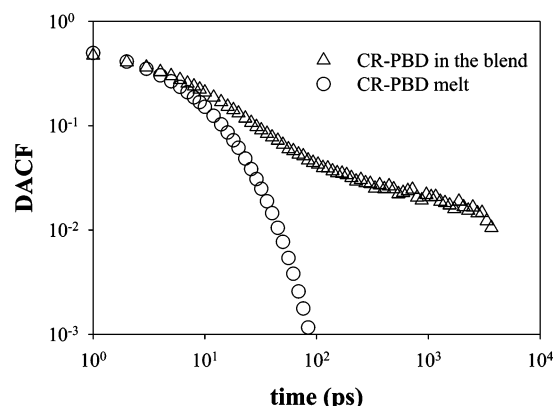


Figure 6. DACFs for the CR-PBD in the neat melt and in the CR-PBD/HFR-PBD blend with 10% of the CR-PBD at 500 K.

broad process in the frequency range that overlaps the response of the CR-PBD component in the blend. Hence, upon blending the high-frequency process (β -relaxation) of the LB-PBD component is only weakly affected while the low-frequency α -relaxation moves to much lower frequencies and broadens significantly. For the CR-PBD component the dielectric loss upon blending becomes narrower and shifts to higher frequencies. Finally, for the total blend the dielectric response consists of two clear peaks: (1) a low-frequency peak due to relaxation of the CR-PBD component and α -process of the LB-PBD component and (2) a high-frequency peak due to β -process of the LB-PBD component.

C. High-Temperature Regime. Results for the FR-PBD/CR-PBD and LB-PBD/CR-PBD blends discussed above clearly show that blending with a slow component differently influences the α - and β -relaxations of the fast component enhancing their (already existing in the pure melt) separation. To determine whether blending with a slow component can promote separation between α - and β -relaxations at temperatures where the pure melt of the fast component exhibits only a single combined process (e.g., as observed from dielectric relaxation), we studied a CR-PBD/HFR-PBD blend with 10% of the CR-PBD component at 500 K. In this blend, the CR-PBD is the fast component while the HFR-PBD matrix is slower (e.g., relaxation time of the α -relaxation) by several orders of magnitude. The CR-PBD melt shows one combined dielectric relaxation process at 500 K as exhibited by the relatively featureless DACF shown in Figure 6. However, when the CR-PBD chains are mixed with much slower HFR-PBD matrix, clear splitting between α - and β -relaxations can be observed as illustrated in Figure 6, resulting in a two-peak dielectric loss of the CR-PBD component in this blend. Note that at this high-temperature most of the relaxation of the DACF of the CR-PBD component in the blend occurs through the β -relaxation which largely follows the combined process in the CR-PBD melt. Therefore, while the dielectric loss associated with the CR-PBD α -relaxation shifts significantly to lower frequencies upon blending, the strong high-temperature β -relaxation, which is weakly influenced by blending, dominates dielectric response of the CR-PBD component.

IV. Discussion and Relation to Experiments

The above analyses of the influence of blending on relaxation processes in a minority fast component of

model miscible blends allow us to make several important observations regarding relaxation mechanisms that we believe have not been considered before in the interpretation of experimental data on miscible polymer blends. First, we observe that blending with a significantly slower component promotes separation between the α - and β -relaxations of the segmental relaxation of the fast component under conditions where those processes are either resolvable or merged in the pure fast component melt. Second, the β -relaxation of the fast component is at most only weakly affected by blending while the α -relaxation of the fast component exhibits a strong concentration dependence of relaxation times. Hence, we interpret the high-frequency loss observed in numerous dielectric spectroscopy studies of miscible polymer blends (see Introduction) that is apparently uninfluenced by blending as being due to the intrinsic β -relaxation of the fast component and not due to concentration fluctuations and/or structural heterogeneities within the blend. In other words, instead of assuming that some fraction of the fast component is not affected upon blending due to presence of the pure meltlike local environments, we believe that a *fraction of the relaxation* of the fast component (the β -relaxation) is not affected by blending and contributes *homogeneously* to the high-frequency response of the blend, while the contribution from the α -relaxation is shifted to lower frequencies with increasing fraction of the slow component.

Finally, we note that when techniques such as NMR spin-lattice relaxation or QENS are employed, measurements are often made at temperatures that are well above the glass transition temperature of the fast component. This is required to move the segmental relaxation time of the fast component into the experimental time window. At these temperatures, the β -relaxation can dominate the merged or nearly merged segmental relaxation.^{21,22} We speculate, therefore, that NMR spin-lattice and QENS measurements may be primarily sensitive to the β -relaxation of the fast component relaxation in some blends and may not detect, or only partially detect, contributions from the composition-dependent α -relaxation of the fast component that may be fairly weak at temperatures above the T_g of the fast component. As a result, these techniques may yield an anomalously weak (apparent) composition dependence of the segmental relaxation time for the fast component on blend composition by associating the segmental relaxation time with the relatively matrix-insensitive β -relaxation and not the composition-dependent α -relaxation of the fast component. For example, this could be the reason for the reported apparent weak composition dependence of the poly(ethylene oxide) segmental relaxations in the poly(ethylene oxide)/poly(methyl methacrylate) blend measured by the spin-lattice NMR.²⁸ On the other hand, this supposition is based on simulations of relatively ideal model polymer blend which does not possess several characteristics (e.g., mismatch in chemical structure of two components, presence of side groups, specific interaction or hydrogen bonding between components, etc.) that have been considered as potentially important factors defining dynamical relaxations in realistic blends.

Acknowledgment. The authors acknowledge Professor Mark Ediger for useful discussions.

References and Notes

- (1) Kumar, S. K.; Colby, R. H.; Anastasiadis, S. H.; Fytas, G. *J. Chem. Phys.* **1996**, *105*, 3777.
- (2) Pathak, J. A.; Colby, R. H.; Floudas, G.; Jerome, R. *Macromolecules* **1999**, *32*, 2553.
- (3) Cendoya, I.; Alegria, A.; Alberdi, J. M.; Colmenero, J.; Grimm, H.; Richter, D.; Frick, B. *Macromolecules* **1999**, *32*, 4065.
- (4) Alvarez, F.; Alegria, A.; Colmenero, J. *Macromolecules* **1997**, *30*, 597.
- (5) Kamath, S.; Colby, R. H.; Kumar, S. K.; Karatasos, K.; Floudas, G.; Fytas, G. *J. Chem. Phys.* **1999**, *111*, 6121.
- (6) Arbe, A.; Alegria, A.; Colmenero, J.; Hoffmann, S.; Willner, L.; Richter, D. *Macromolecules* **1999**, *32*, 7572.
- (7) Chung, G.-C.; Kornfield, J. A.; Smith, S. D. *Macromolecules* **1994**, *27*, 964. Chung, G.-C.; Kornfield, J. A.; Smith, S. D. *Macromolecules* **1994**, *27*, 5729.
- (8) Zetsche, A.; Fischer, E. W. *Acta Polym.* **1994**, *45*, 168.
- (9) Lodge, T. P.; McLeish, T. C. B. *Macromolecules* **2000**, *33*, 5278.
- (10) Colby, R. H.; Lipson, J. E. *Macromolecules* **2005**, *38*, 4919.
- (11) Adam, G.; Gibbs, J. H. *J. Chem. Phys.* **1965**, *43*, 139.
- (12) He, Y.; Lutz, T. R.; Ediger, M. D. *J. Chem. Phys.* **2003**, *119*, 9956.
- (13) Leroy, E.; Alegria, A.; Colmenero, J. *Macromolecules* **2003**, *36*, 7280.
- (14) Smith, G. D.; Paul, W. *J. Phys. Chem. A* **1998**, *102*, 1200.
- (15) Smith, G. D.; Borodin, O.; Bedrov, D.; Paul, W.; Qiu, X. H.; Ediger, M. D. *Macromolecules* **2001**, *34*, 5192.
- (16) Smith, G. D.; Paul, W.; Monkenbusch, M.; Richter, D. *Chem. Phys.* **2000**, *261*, 61. Smith, G. D.; Paul, W.; Monkenbusch, M.; Richter, D. *J. Chem. Phys.* **2001**, *114*, 4285.
- (17) Smith, G. D.; Borodin, O.; Paul, W. *J. Chem. Phys.* **2002**, *117*, 10350.
- (18) Krushev, S.; Paul, W.; Smith, G. D. *Macromolecules* **2002**, *35*, 4198.
- (19) The temperature at which the relaxation time for the torsional autocorrelation function is 1 s.
- (20) Ryckaert, J.; Ciccotti, G.; Berendsen, H. J. C. *J. Comput. Phys.* **1977**, *23*, 327–341.
- (21) Bedrov, D.; Smith, G. D. *Phys. Rev. E* **2005**, *71*, 050801(R) (1–4).
- (22) Smith, G. D.; Bedrov, D. *J. Non-Cryst. Solids*, submitted for publication.
- (23) Kohlrausch, F. *Pogg. Ann. Phys.* **1863**, *119*, 352. Williams, G.; Watts, D. C. *Trans. Faraday Soc.* **1970**, *66*, 80.
- (24) Williams, G. *Adv. Polym. Sci.* **1979**, *33*, 60.
- (25) Arbe, A.; Richter, D.; Colmenero, J.; Farago, B. *Phys. Rev. E* **1996**, *54*, 3853.
- (26) Edwards, D. M. F.; Madden, P. A.; McDonald, I. R. *Mol. Phys.* **1984**, *51*, 1141.
- (27) Smith, G. D.; Paul, W.; Monkenbusch, M.; Willner, L.; Richter, D.; Qiu, X. H.; Ediger, M. D. *Macromolecules* **1999**, *32*, 8857.
- (28) Lutz, T. R.; He, Y.; Ediger, M. D.; Cao, H.; Lin, G.; Jones, A. A. *Macromolecules* **2003**, *36*, 1724.

MA0517392